Letter

Universal entanglement signatures of interface conformal field theories

Qicheng Tang,[1,2,*] Zixia Wei,[3,4,*] Yin Tang,[1,2] Xueda Wen,[5,6] and W. Zhu[1,2,†]
[1]Department of Physics, School of Science, Westlake University, Hangzhou 310030, China
[2]Institute of Natural Sciences, Westlake Institute for Advanced Study, Hangzhou 310024, China
[3]Yukawa Institute for Theoretical Physics, Kyoto University, Kyoto 606-8502, Japan
[4]Interdisciplinary Theoretical and Mathematical Sciences Program (iTHEMS), RIKEN, Wako 351-0198, Japan
[5]Department of Physics, Harvard University, Cambridge, Massachusetts 02138, USA
[6]Department of Physics, University of Colorado, Boulder, Colorado 80309, USA

(Received 18 August 2023; revised 27 November 2023; accepted 13 December 2023; published 8 January 2024)

An interface connecting two distinct conformal field theories hosts rich critical behaviors. In this paper, we investigate the entanglement properties of such critical interface theories for probing the underlying universality. As inspired by holographic perspectives, we demonstrate vital features of various entanglement measures regarding such interfaces based on several paradigmatic lattice models. Crucially, for two subsystems adjacent at the interface, the mutual information and the reflected entropy exhibit identical leading logarithmic scaling, giving an effective interface central charge that takes the same value as the smaller central charge of the two conformal field theories. Our paper demonstrates that the entanglement measure offers a powerful tool to explore the rich physics in critical interface theories.

DOI: 10.1103/PhysRevB.109.L041104

Entanglement offers an exotic path to characterize the universal information about conformal symmetry at quantum critical points [1–6]. Especially, when conformal symmetry is partially broken by boundaries and defects into a subset, entanglement is sensitive to their presence and can capture their intrinsic features [7–14]. In this Letter, we explore an interface gluing two distinct conformal field theories (CFTs) with different values of the central charge: $c^{(\mathrm{I})}$ for CFT$^{(\mathrm{I})}$ and $c^{(\mathrm{II})}$ for another CFT$^{(\mathrm{II})}$, and focus on possible universal entanglement signatures about the interface. Such kinds of interfaces can naturally appear in various scenarios, like the junction of two quantum wires [15,16], renormalization group (RG) interfaces between QFTs [17–22], and evaporation of black holes [23–25], just to name a few.

When two CFTs are glued in a scale-invariant way [26], the theory is called an *interface CFT* (ICFT). Existing attempts on ICFT are mainly based on a simple folding picture [26–28] which converts the interface to a boundary condition of the folded theory. While this tool is powerful for investigating two-point functions and transmission properties, the entanglement properties are, in general, not under analytical control and more difficult to access [29–34], especially for our interested case of $c^{(\mathrm{I})} \neq c^{(\mathrm{II})}$. This problem is particularly challenging in the context of CFT, and therefore motivates us to consider a holographic estimation and lattice simulations.

Here, we consider two distinct CFTs with the same length L glued into a circle with length $2L$ through an interface. To access the entanglement structure of its ground state, we start by investigating a holographic thin-brane model [25,35–41] for realizing ICFT$_2$. While such a construction is extremely special, it might be the simplest example of ICFTs with nontrivial interfaces whose entanglement properties are analytically tractable. Based on the insights from the holographic ICFT, we numerically study two paradigmatic lattice models. As shown in Fig. 1(a), a symmetric entanglement-cut configuration allows us to extract universal information about the interface. In particular, we uncover a selection rule of an effective interface central charge $c_{\mathrm{eff}} = \min\{c^{(\mathrm{I})}, c^{(\mathrm{II})}\}$ from the reflected entropy (RE), which offers a peek into the underlying physics of interface.

Insights from AdS/ICFT. The gravity dual of a holographic ICFT$_2$ can be constructed in a bottom-up fashion using the thin brane model [25,40,42]. As shown in Figs. 1(b) and 1(c), two 3D anti–de Sitter (AdS$_3$) spacetime $\mathcal{M}^{(\mathrm{I})}$ and $\mathcal{M}^{(\mathrm{II})}$ with different AdS radii $\alpha^{(\mathrm{I})}$ and $\alpha^{(\mathrm{II})}$ are joined on a tensile brane Q, to mimic an ICFT$_2$ of gluing two distinct CFTs. The AdS radii on the gravity side and the central charges on the ICFT$_2$ side are related by [43]

$$c^{(\mathrm{I,II})} = 3\alpha^{(\mathrm{I,II})}/2G_N, \tag{1}$$

where G_N is the Newton constant, and we let $c^{(\mathrm{I})} < c^{(\mathrm{II})}$ in the following. Meanwhile, the location of the brane Q is determined by solving a junction condition between $\mathcal{M}^{(\mathrm{I})}$ and $\mathcal{M}^{(\mathrm{II})}$, which reflects nontrivial interaction between CFT$^{(\mathrm{I})}$ and CFT$^{(\mathrm{II})}$. For a discussion on the standard AdS/CFT correspondence and the thin-brane model for realizing ICFT$_2$, see Supplemental Material [44] and also Refs. [25,45–48].

The holographic ICFT$_2$ can be considered to be living on the asymptotic boundary of the current AdS$_3$ setup. In AdS/ICFT, the EE for a subsystem A in the ICFT can be computed from the length of the geodesic γ_A which connects

*These authors contributed equally to this work.
†zhuwei@westlake.edu.cn

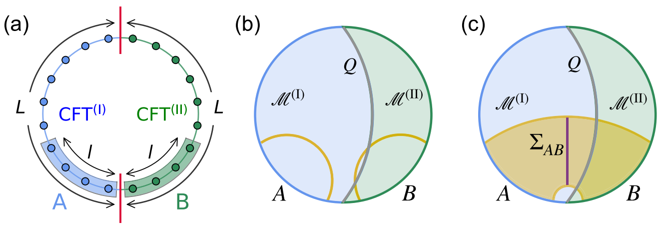

FIG. 1. A schematic of ICFT and the corresponding holographic model. (a) Two distinct CFTs with length L are glued into an ICFT on a circle with length $2L$. Two subsystems A (blue shade) and B (green shade) are located on two sides of the interface (red). (b), (c) The thin-brane model for realizing a holographic ICFT_2 contains two AdS_3 manifolds $\mathcal{M}^{(\mathrm{I})}$ and $\mathcal{M}^{(\mathrm{II})}$ with different AdS radii $\alpha^{(\mathrm{I})}$ and $\alpha^{(\mathrm{II})}$ joined by a 2D thin brane Q in gray. For convenience, we let $c^{(\mathrm{I})} < c^{(\mathrm{II})}$, and hence $\alpha^{(\mathrm{I})} < \alpha^{(\mathrm{II})}$. Yellow lines in (b) represent the RT surface of A/B for calculating the holographic EE, and purple line in (c) is the entanglement-wedge cross section Σ_{AB} of A and B.

the endpoints of A as [49,50]

$$S_A = \frac{\mathrm{Length}(\gamma_A)}{4G_N}. \tag{2}$$

Here, γ_A is called the Ryu-Takayanagi (RT) surface of A. Figure 1(b) shows what the RT surfaces look like for a single interval A in $\mathcal{M}^{(\mathrm{I})}$ and a single interval B in $\mathcal{M}^{(\mathrm{II})}$. Note that it is possible for an RT surface to penetrate the brane, which results in a diverse behavior of the EE. However, for an interval A living in $\mathrm{CFT}^{(\mathrm{I})}$, γ_A always lies inside $\mathcal{M}^{(\mathrm{I})}$ and we find

$$\begin{aligned} S_{A\in \mathrm{CFT}^{(\mathrm{I})}} &= \frac{c^{(\mathrm{I})}}{3} \ln\left(\frac{2L}{\pi\epsilon}\sin\left(\frac{\pi l}{2L}\right)\right) \\ &= \frac{c^{(\mathrm{I})}}{3}\ln\frac{l}{\epsilon} + \mathcal{O}\left(\left(\frac{l}{L}\right)^2\right), \end{aligned} \tag{3}$$

where l is the length of A and ϵ is a UV cutoff corresponding to the lattice distance. We can also get a clean result when A is an interval with length $2l$ and is symmetric with respect to the interface. Let us call the EE in this case the *symmetric EE*, and it turns out to be

$$S_{\mathrm{symm}} = \frac{c^{(\mathrm{I})}+c^{(\mathrm{II})}}{6}\ln\left(\frac{2L}{\pi\epsilon}\sin\left(\frac{\pi l}{L}\right)\right) + \mathrm{const}. \tag{4}$$

This relation is not only accessible via a holographic calculation but also can be derived by using the folding trick and the Cardy-Tonni approach [51] in the context of CFT, see details in Supplemental Material [44].

Another useful correlation measure that reflects entanglement structures to study is the RE. Initially proposed in the context of AdS/CFT [52], the RE has attracted considerable attention [53–63]. For a (generally mixed) state ρ_{AB} on subsystem $A\cup B$, we can diagonalize it as $\rho_{AB} = \sum_i p_i|\varphi_i\rangle\langle\varphi_i|$. The canonical purification of ρ_{AB} is accordingly defined as $|\sqrt{\rho_{AB}}\rangle = \sum_i \sqrt{p_i}|\varphi_i\rangle|\varphi_i^*\rangle$, where for each $|\varphi_i\rangle \in \mathcal{H}_A\otimes\mathcal{H}_B$, $|\varphi_i^*\rangle \in \mathcal{H}_{A^*}\otimes\mathcal{H}_{B^*}$ is its CPT conjugate. The RE between A and B is defined as the EE of the canonical purification:

$$S^R_{A:B} = S_{AA^*}(|\sqrt{\rho_{AB}}\rangle). \tag{5}$$

Notably, as shown in Fig. 1(c), in holographic theories, RE can also be computed geometrically as [52]

$$S^R_{A:B} = \frac{2\mathrm{Length}(\Sigma_{AB})}{4G_N}, \tag{6}$$

where Σ_{AB} is the minimal surface crossing the region surrounded by the entanglement wedge [64–66] $\gamma_{AB}\cup A\cup B$ of subsystem $A\cup B$, so-called the entanglement-wedge cross-section [52,56,67–70]. For two adjacent subsystems A and B with size $l = l_A = l_B$ that touch at the interface, Σ_{AB} always locates inside $\mathcal{M}^{(\mathrm{I})}$ and one finds [40,44]

$$\begin{aligned} S^R_{A:B} &= \frac{c^{(\mathrm{I})}}{3}\ln\left(\frac{2L}{\pi\epsilon}\tan\left(\frac{\pi l}{2L}\right)\right) \\ &= \frac{\min\{c^{(\mathrm{I})},c^{(\mathrm{II})}\}}{3}\ln\frac{l}{\epsilon} + \mathcal{O}\left(\left(\frac{l}{L}\right)^2\right), \end{aligned} \tag{7}$$

which depends only on the smaller central charge. Note that, compared to previous results [25,39–41] where the setups were on an infinite line, we present the very first analysis of holographic entanglement entropy in holographic ICFT defined on a compact space constructed by the thin-brane model. Although we have just presented analytic formulas for some special choices of the subsystem, results for generic subsystems can be found in Supplemental Material [44]. In the analysis for generic subsystems, taking into account the nontrivial saddle points, where the RT surface crosses the thin-brane twice [25], turns out to be very important.

Below, we will introduce two paradigmatic lattice models and numerically test if the behaviors observed above also hold in them. Before proceeding, we would like to note that, while it is natural to expect that Eq. (4) holds generically [39], it would be very surprising to find Eqs. (3) and (7) hold in generic cases. To see this, we may consider a trivial ICFT with no interaction between $\mathrm{CFT}^{(\mathrm{I})}$ and $\mathrm{CFT}^{(\mathrm{II})}$. In this case, for an interval A lying in $\mathrm{CFT}^{(\mathrm{I})}$ and ending at the interface, the leading order of S_A would be $(c^{(\mathrm{I})}/6)\ln l$, which is roughly half of Eq. (3). As for the RE, since $\rho_{AB} = \rho_A\otimes\rho_B$ in this case, $S^R_{A:B}$ would be zero which differs a lot from Eq. (7). On the other hand, Eq. (4) still holds. Therefore, up to this point, it is natural to expect that Eqs. (3) and (7) reflect the uniqueness of the interface interaction exhibiting in AdS/ICFT. However, surprisingly, we will see that all of Eqs. (3), (4), and (7) hold in the lattice models studied below, which suggests that they may generically hold in nontrivial ICFTs.

Lattice models and numerical method. In what follows, we consider two lattice models for realizing ICFT_2. The first one is the O'Brien-Fendley (OF) model [71] with an inhomogeneous coupling constant

$$H_1 = H_{\mathrm{TFI}} + g_L\sum_{n\leqslant -1} H_{\mathrm{int}}(n) + g_R\sum_{n\geqslant 0} H_{\mathrm{int}}(n), \tag{8}$$

where $H_{\mathrm{TFI}} = \sum_n \sigma^x_n\sigma^x_{n+1} - \sigma^z_n$, $H_{\mathrm{int}} = \sigma^x_{n-1}\sigma^x_n\sigma^z_{n+1} + \sigma^z_{n-1}\sigma^x_n\sigma^x_{n+1}$, and the site index n run over $[-L, L-1]$. The anisotropy between g_L and g_R creates an interface at the bond connecting spins at site -1 and site 0. Since we are considering a periodic chain, there is another symmetric interface bond between site $-L$ and site $L-1$. In the homogeneous case of $g = g_L = g_R$, the OF model realizes a

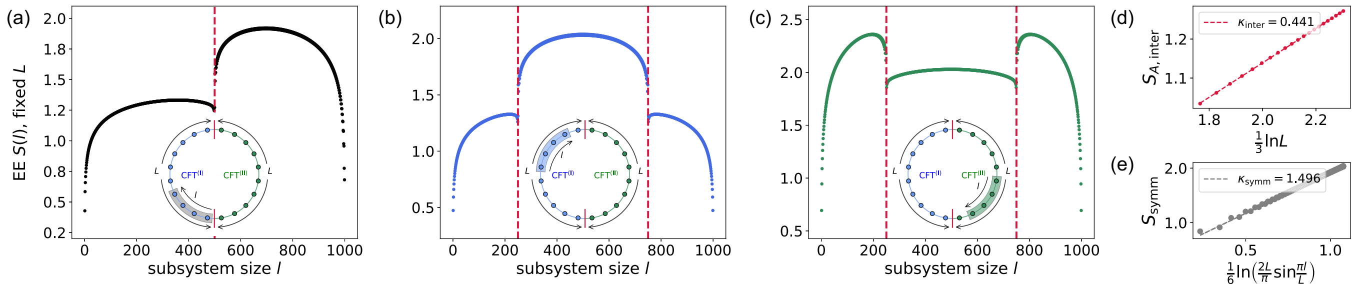

FIG. 2. The bipartite EE in a fermionic model of gluing the real fermion CFT ($c^{(\mathrm{I})} = \frac{1}{2}$) at left and the complex fermion CFT ($c^{(\mathrm{II})} = 1$) at right, under a periodic boundary condition. (a)–(c) The dependence of EE on the subsystem size l, with fixed total system size $2L = 1000$. The insets show corresponding entanglement-cut configurations: fix one end (a) at the interface, (b) in the middle of CFT$^{(\mathrm{I})}$, and (c) in the middle of CFT$^{(\mathrm{II})}$. The red dashed lines represent the phase boundaries that one end of the subsystem touches the interface, which hosts a jump on the bulk degrees of freedom. (d) The dependence of EE on the total system size $2L$, where both ends of the subsystem A lie on the interface. (e) The dependence of symmetric EE on the subsystem size l, with fixed total system size $2L = 1000$. These numerical results are consistent with holographic calculations (see Supplemental Material [44]).

tricritical Ising fixed point at $g = g_c$ that separates a phase with Ising universality class for $g < g_c$ and a gapped phase for $g > g_c$.[1]. In the context of CFT, tuning the coupling constant g away from g_c can be understood as adding a $\Phi_{1,3}$ operator that triggers an RG flow from tricritical Ising CFT to Ising CFT or massive IR, depending on the sign of $\Phi_{1,3}$ [72]. Setting $g_L = 0$ and $g_R = g_c$, the lattice Hamiltonian in Eq. (8) offers an appropriate playground for an interface of gluing the Ising CFT at the left part (with $c_1^{(\mathrm{I})} = \frac{1}{2}$) and the tricritical Ising CFT at the right part ($c_1^{(\mathrm{II})} = \frac{7}{10}$).

The second one is a noninteracting fermionic model with inhomogeneous pairing

$$H_2 = \sum_{n\leqslant -1} H_{\mathrm{RF}}(n) + \sum_{n\geqslant 0} H_{\mathrm{CF}}(n), \tag{9}$$

where $H_{\mathrm{RF}}(n) = H_{\mathrm{CF}}(n) + (f_n f_{n+1} + \mathrm{H.c.}) - 2f_n^\dagger f_n$ and $H_{\mathrm{CF}}(n) = -f_n^\dagger f_{n+1} + \mathrm{H.c.}$ Here, the left half chain with pairing terms realizes a real (Majorana) fermion CFT with $c_2^{(\mathrm{I})} = \frac{1}{2}$, but the right half chain realizes a complex (Dirac) fermion CFT with $c_2^{(\mathrm{II})} = 1$. Again, an interface of gluing two distinct CFTs is created between site -1 and site 0. Up to a Jordan-Winger transformation, this model is dual to a spin model of gluing an Ising chain and an XX chain.

For accessing entanglement properties of these lattice models, we perform a numerical simulation based on matrix product states (MPS) techniques [73].[2] First, the ground state of the model is solved by the density matrix renormalization group algorithm [76] with a bond dimension χ. At this step, one can easily obtain the bipartite EE. Second, for calculating mutual information (MI) and RE, we need to evaluate reduced density matrices for a continuous region (the subsystems A, B and their complement $A \cup B$), for which the computational complexity grows exponentially. An efficient simulation requires further compressing the dimension of local Hilbert space of the cutting subsystem (the dimension of reduced density matrix ρ_A) to $\widetilde{d}_A$ by applying a standard MPS coarse-graining procedure to the physical leg of the subsystem's local wave function (see Supplemental Material [44]). Through this approach, we are able to calculate the multipartite entanglement measures—MI and RE with high accuracy and affordable computational complexity: $\chi = 100$ and $\widetilde{d}_A = 100$ for the Hamiltonian in Eqs. (8) and (9) with total system size $2L$ up to 300 under a periodic boundary condition.

Entanglement entropy. Let us begin with inspecting the dependence of EE on the subsystem size. In Fig. 2, we present the result on the fermionic Hamiltonian of Eq. (9), as its noninteracting nature allows an exact solution of the EE (see inhomogeneous OF model in Supplemental Material [44]). Remarkably, we find good agreement between these lattice results and a holographic calculation on the thin-brane model (see Supplemental Material [44]) for various entanglement-cut configurations. The subsystem-size dependence of EE shows a clear change in bulk degrees of freedom across the interface, corresponding to the two distinct bulk central charges on each side of the interface. Moreover, when both ends of the subsystem lie on the interface (subsystem $A = \{-L, -L+1, \cdots, -1\}$), we find that the corresponding EE exhibits a logarithmic scaling $S_{A,\mathrm{inter}} \propto \ln L$, as shown in Fig. 2(d). This provides strong evidence that a massive RG flow is not triggered in our lattice model, while the prefactor of logarithmic EE of cutting along the interface is generally not of universal meaning in the case of CFT$^{(\mathrm{I})} \neq$ CFT$^{(\mathrm{II})}$ [77].

We now try to extract possible universal information about the interface from the finite-size scaling forms obtained from holographic derivation. In the case of cutting a subsystem A in CFT$^{(\mathrm{I})}$, holographic calculation on the thin-brane model gives the result shown in (3), as a pure CFT$^{(\mathrm{I})}$. In lattice simulations, we find that this scaling form is valid at $l \ll L$, even when $A = [-l, -a]$, $a \to 0$ is very close to the interface. Another solvable case is the symmetric EE of cutting a

[1]Theoretically, one can confirm $g_c < 0.5$, but the exact value of g_c can only be numerically obtained and would be modified by finite size or the interface setting. In the homogeneous case, we find the previously reported critical value $g_c \approx 0.428$ in Ref. [71] is faithful, but it is modified in the interface case as $g_c \sim 0.41$ for our considered total system size.

[2]Here we note that the second fermionic model is noninteracting and Gaussian, which allows an exact solution of the EE and MI from the correlation matrix techniques [74,75].

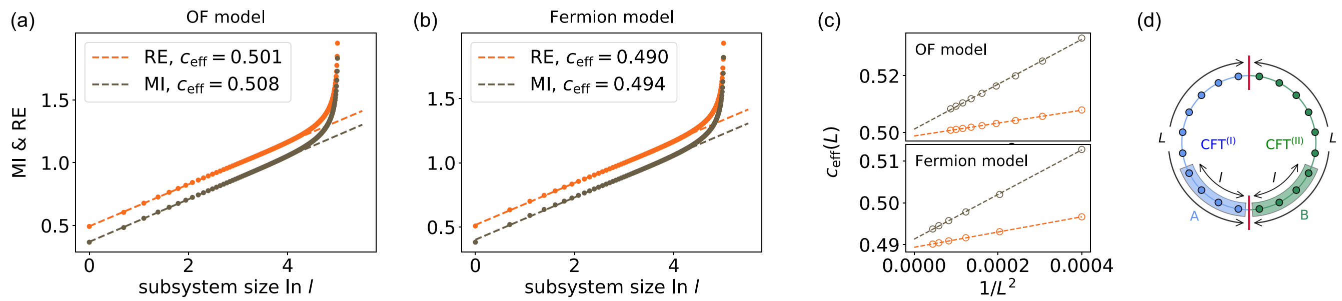

FIG. 3. The scaling behavior of MI $I_{A:B}$ and RE $S^R_{A:B}$ for two adjacent subsystems A and B, of which the touching point is located at the interface, for (a) the inhomogeneous OF model of gluing the Ising CFT ($c^{(\rm I)} = \frac{1}{2}$) and the tricritical Ising CFT ($c^{(\rm II)} = \frac{7}{10}$), and (b) a fermionic model of of gluing the real fermion CFT ($c^{(\rm I)} = \frac{1}{2}$) and the complex fermion CFT ($c^{(\rm II)} = 1$), with total system size $2L = 300$. The dashed lines represent linear fits in the form of $S^R_{A:B} \sim I_{A:B} = \frac{c_{\rm eff}}{3} \ln l + b$ under $l \ll L$. (c) A finite-size scaling of the extracted $c_{\rm eff}(L)$ from RE and MI, under various total system size $2L \in [100, 300]$. The dashed lines represent linear fits in the form of $c_{\rm eff}(L) = k/L^2 + c_{\rm eff}(L \to \infty)$, giving $c_{\rm eff,1}(L \to \infty, \text{MI}) \approx 0.501$, $c_{\rm eff,1}(L \to \infty, \text{RE}) \approx 0.499$ for the OF model and $c_{\rm eff,2}(L \to \infty, \text{MI}) \approx 0.491$, $c_{\rm eff,2}(L \to \infty, \text{RE}) \approx 0.489$ for the fermionic model. (d) A schematic of the entanglement-cut configuration, where two adjacent subsystems A and B with the same length l touch at the interface.

subsystem $A = [-l, l]$ that is symmetrically around the interface at $x = 0$. Holographic calculation suggests the scaling form in a finite system is given by (4). This scaling form also appears in numerical simulation on lattice models with high accuracy [see Fig. 2(e)]. For characterizing the interface, one may consider extracting the interface entropy (see Supplemental Material [44] for a definition) from lattice simulations. However, different from the case of gluing two identical CFTs [31,32,34,78,79], here we do not have a simple way to separate the interface entropy from the nonuniversal correction in the subleading term of EE. Moreover, it is worth noting that the discussion in this section focuses on the logarithmic dependence of EE on the subsystem size l. This is, in general, different from considering the logarithmic dependence on the UV cutoff ϵ, for which a universal relation of the prefactor is expected [39,41,80].

Reflected entropy and mutual information. Let us then move on to study the RE and MI. In pure CFTs, a symmetric entanglement-cut configuration of separating two adjacent subsystems A and B with the same length l leads to $S^R_{A:B} \sim I_{A:B} \sim \frac{c}{3} \ln l$. By putting the touching point of A and B onto the interface (see a schematic in Fig. 3), holographic calculation suggests that the RE remains the same logarithmic scaling in ICFTs, as shown in Eq. (7). The only difference appears in the prefactor with replacing the central charge c to an effective value $c_{\rm eff} = \min\{c^{(\rm I)}, c^{(\rm II)}\}$. While this behavior was observed in a simple thin-brane model, we will see that, surprisingly, it also precisely holds in both of the two lattice models considered here.

As shown in Figs. 3(a) and 3(b), for a given finite total system size $2L$, the RE $S^R_{A:B}$ exhibits a logarithmic dependence on l. A further finite-size scaling [see Fig. 3(c)] on the prefactor of logarithmic RE suggests $c_{\rm eff,1} \approx 0.499$, approaching $\min\{\frac{1}{2}, \frac{7}{10}\}$, and $c_{\rm eff,2} \approx 0.489$, approaching $\min\{\frac{1}{2}, 1\}$, in the thermodynamic limit $L \to \infty$. Moreover, holographic calculation implies that the MI $I_{A:B} = S_A + S_B - S_{AB}$ (and, consequently, the Markov gap $S^R_{A:B} - I_{A:B}$ [81]) in ICFTs has a convoluted dependence on the subsystem size l, since S_B involves a nontrivial phase of EE scaling (see details in Supplemental Material [44]). Numerically, we also find that the RE and MI exhibit distinct scaling behaviors on the subsystem size l when l becomes comparable with the total system size $2L$. Nevertheless, we behold a logarithmic MI $I_{A:B} \sim \frac{c'_{\rm eff}}{3} \ln l$ under $l \ll L$, sharing the same selection rule of $c_{\rm eff} = c'_{\rm eff} = \min\{c^{(\rm I)}, c^{(\rm II)}\}$ [a finite-size scaling gives $c'_{\rm eff,1}(L \to \infty) \approx 0.501$ on the OF model and $c'_{\rm eff,2} \approx 0.491$ on the fermion model]. To summarize, we conclude that there is a universal scaling of tripartite entanglement measure in critical interface theories as $S^R_{A:B} \sim I_{A:B} \sim \frac{c_{\rm eff}}{3} \ln l$, with a single effective central charge satisfying the universal selection rule of $c_{\rm eff} = \min\{c^{(\rm I)}, c^{(\rm II)}\}$.

Discussions and outlooks. We have explored possible universal entanglement signatures in ICFTs through numerical simulations on the representative lattice models. Some initiations were provided from a holographic perspective by considering a simple brane construction in AdS_3 to mimic the ICFT_2. Surprisingly, numerical results obtained from lattice models resemble a lot of observations in AdS/ICFT. One of the most important features is that the effective central charge appearing in the RE is given by $c_{\rm eff} = \min\{c^{(\rm I)}, c^{(\rm II)}\}$.

These common features between lattice models and AdS/ICFT are surprising because they do not hold, in general, ICFTs, and one can easily construct a counterexample, e.g., by considering an ICFT without interaction between the two sides. In general, the value of $\frac{1}{3}\min\{c^{(\rm I)}, c^{(\rm II)}\}$ is expected to be the upper bound for the prefactor of RE, and the condition of saturating it is not clear. Intuitively, saturating the upper bound requires (almost) perfect transmission associate with the interface. On lattice models, this means that we should let the (dominate) bond coupling at the interface take the same value as in the bulk of the connected two half-spaces. Otherwise, the transmission rate of the interface would be strongly reduced. Both of the two considered lattice models are constructed based on this consideration. Moreover, it is tested that local perturbations on the interface do not lead to a qualitative change of the universal logarithmic scaling of MI and RE, which indicates an RG stability of our critical theories. It motivates us to conjecture that the observed features are universal for a class of critical interface theories with an RG stability, which needs further study to demonstrate.

Moreover, we would like to point out that the inhomogeneous OF model realizes a specific case of *RG interfaces* between nearby minimal models (tricritical Ising CFT at UV and Ising CFT at IR) [18,22]. Universal information about the RG flow is expected to be traceable through two-point correlations [17–19,22], which was investigated by a recent work [82] with introducing a different lattice model. Our results are potentially helpful for extracting this information from the entanglement structure. Another free fermionic interface model provides a particular approach to study symmetry breaking in ICFTs, where the $U(1)$ symmetry of Dirac fermion is broken to Z_2 of Majorana fermion on half-space. In addition, it would also be interesting to explore other interface models with more complicated structures, e.g., an interface separating a unitary CFT from a nonunitary CFT (e.g., Ising to Lee-Yang fixed point [29,83]). We leave these to future investigations.

Acknowledgments. We thank Y. Kusuki, M. Nozaki, and S.-M. Ruan for discussion. We also thank H. Geng, A. Karch, Z.-X. Luo, C. Uhlemann, and M. Wang for valuable comments on a draft of this paper. W.Z. was supported by the Key R&D Program of Zhejiang Province under No. 2022SDXHDX0005, No. 2021C01002, the National Key R&D Program under No. 2022YFA1402200, and NSFC under No. 92165102. Z.W. was supported by Grant-in-Aid for JSPS Fellows No. 20J23116. X.W. is supported by the Simons Collaboration on Ultra-Quantum Matter (UQM), which is funded by grants from the Simons Foundation (No. 651440 and No. 618615).

[1] C. Holzhey, F. Larsen, and F. Wilczek, Geometric and renormalized entropy in conformal field theory, Nucl. Phys. B **424**, 443 (1994).
[2] G. Vidal, J. I. Latorre, E. Rico, and A. Kitaev, Entanglement in quantum critical phenomena, Phys. Rev. Lett. **90**, 227902 (2003).
[3] P. Calabrese and J. Cardy, Entanglement entropy and quantum field theory, J. Stat. Mech. (2004) P06002.
[4] E. Fradkin and J. E. Moore, Entanglement entropy of 2D conformal quantum critical points: Hearing the shape of a quantum drum, Phys. Rev. Lett. **97**, 050404 (2006).
[5] B. Hsu, M. Mulligan, E. Fradkin, and E.-A. Kim, Universal entanglement entropy in two-dimensional conformal quantum critical points, Phys. Rev. B **79**, 115421 (2009).
[6] P. Bueno, R. C. Myers, and W. Witczak-Krempa, Universality of corner entanglement in conformal field theories, Phys. Rev. Lett. **115**, 021602 (2015).
[7] N. Laflorencie, E. S. Sørensen, M.-S. Chang, and I. Affleck, Boundary effects in the critical scaling of entanglement entropy in 1D systems, Phys. Rev. Lett. **96**, 100603 (2006).
[8] H.-Q. Zhou, T. Barthel, J. O. Fjærestad, and U. Schollwöck, Entanglement and boundary critical phenomena, Phys. Rev. A **74**, 050305(R) (2006).
[9] E. S. Sørensen, M.-S. Chang, N. Laflorencie, and I. Affleck, Quantum impurity entanglement, J. Stat. Mech. (2007) P08003.
[10] E. S. Sørensen, M.-S. Chang, N. Laflorencie, and I. Affleck, Impurity entanglement entropy and the Kondo screening cloud, J. Stat. Mech. (2007) L01001.
[11] I. Affleck, N. Laflorencie, and E. S. Sørensen, Entanglement entropy in quantum impurity systems and systems with boundaries, J. Phys. A: Math. Theor. **42**, 504009 (2009).
[12] F. Iglói, Z. Szatmári, and Y.-C. Lin, Entanglement entropy with localized and extended interface defects, Phys. Rev. B **80**, 024405 (2009).
[13] R. Vasseur, J. L. Jacobsen, and H. Saleur, Universal entanglement crossover of coupled quantum wires, Phys. Rev. Lett. **112**, 106601 (2014).
[14] C. P. Herzog, K.-W. Huang, and K. Jensen, Universal entanglement and boundary geometry in conformal field theory, J. High Energy Phys. 01 (2016) 162.
[15] N. Sedlmayr, D. Morath, J. Sirker, S. Eggert, and I. Affleck, Conducting fixed points for inhomogeneous quantum wires: A conformally invariant boundary theory, Phys. Rev. B **89**, 045133 (2014).
[16] Y.-T. Kang, C.-Y. Lo, M. Oshikawa, Y.-J. Kao, and P. Chen, Two-wire junction of inequivalent Tomonaga-Luttinger liquids, Phys. Rev. B **104**, 235142 (2021).
[17] I. Brunner and D. Roggenkamp, Defects and bulk perturbations of boundary Landau-Ginzburg orbifolds, J. High Energy Phys. 04 (2008) 001.
[18] D. Gaiotto, Domain walls for two-dimensional renormalization group flows, J. High Energy Phys. 12 (2012) 103.
[19] A. Konechny and C. Schmidt-Colinet, Entropy of conformal perturbation defects, J. Phys. A: Math. Theor. **47**, 485401 (2014).
[20] I. Brunner and C. Schmidt-Colinet, Reflection and transmission of conformal perturbation defects, J. Phys. A: Math. Theor. **49**, 195401 (2016).
[21] J. Cardy, Bulk renormalization group flows and boundary states in conformal field theories, SciPost Phys. **3**, 011 (2017).
[22] A. Konechny, Properties of RG interfaces for 2D boundary flows, J. High Energy Phys. 05 (2021) 178.
[23] H. Z. Chen, R. C. Myers, D. Neuenfeld, I. A. Reyes, and J. Sandor, Quantum extremal islands made easy. Part I. Entanglement on the brane, J. High Energy Phys. 10 (2020) 166.
[24] H. Z. Chen, R. C. Myers, D. Neuenfeld, I. A. Reyes, and J. Sandor, Quantum extremal islands made easy. Part II. Black holes on the brane, J. High Energy Phys. 12 (2020) 025.
[25] T. Anous, M. Meineri, P. Pelliconi, and J. Sonner, Sailing past the end of the world and discovering the island, SciPost Phys. **13**, 075 (2022).
[26] C. Bachas, J. de Boer, R. Dijkgraaf, and H. Ooguri, Permeable conformal walls and holography, J. High Energy Phys. 06 (2002) 027.
[27] E. Wong and I. Affleck, Tunneling in quantum wires: A boundary conformal field theory approach, Nucl. Phys. B **417**, 403 (1994).
[28] M. Oshikawa and I. Affleck, Boundary conformal field theory approach to the critical two-dimensional Ising model with a defect line, Nucl. Phys. B **495**, 533 (1997).
[29] T. Quella, I. Runkel, and G. M. Watts, Reflection and transmission for conformal defects, J. High Energy Phys. 04 (2007) 095.
[30] K. Sakai and Y. Satoh, Entanglement through conformal interfaces, J. High Energy Phys. 12 (2008) 001.

[31] I. Peschel and V. Eisler, Exact results for the entanglement across defects in critical chains, J. Phys. A: Math. Theor. **45**, 155301 (2012).
[32] P. Calabrese, M. Mintchev, and E. Vicari, Entanglement entropy of quantum wire junctions, J. Phys. A: Math. Theor. **45**, 105206 (2012).
[33] V. Eisler and I. Peschel, On entanglement evolution across defects in critical chains, Europhys. Lett. **99**, 20001 (2012).
[34] E. Brehm and I. Brunner, Entanglement entropy through conformal interfaces in the 2D Ising model, J. High Energy Phys. 09 (2015) 080.
[35] J. Erdmenger, M. Flory, and M.-N. Newrzella, Bending branes for DCFT in two dimensions, J. High Energy Phys. 01 (2015) 058.
[36] P. Simidzija and M. Van Raamsdonk, Holo-ween, J. High Energy Phys. 12 (2020) 028.
[37] C. Bachas, S. Chapman, D. Ge, and G. Policastro, Energy reflection and transmission at 2D holographic interfaces, Phys. Rev. Lett. **125**, 231602 (2020).
[38] C. Bachas and V. Papadopoulos, Phases of holographic interfaces, J. High Energy Phys. 04 (2021) 262.
[39] A. Karch, Z.-X. Luo, and H.-Y. Sun, Universal relations for holographic interfaces, J. High Energy Phys. 09 (2021) 172.
[40] Y. Kusuki, Reflected entropy in boundary and interface conformal field theory, Phys. Rev. D **106**, 066009 (2022).
[41] A. Karch and M. Wang, Universal behavior of entanglement entropies in interface CFTs from general holographic spacetimes, J. High Energy Phys. 06 (2023) 145.
[42] T. Azeyanagi, T. Takayanagi, A. Karch, and E. G. Thompson, Holographic calculation of boundary entropy, J. High Energy Phys. 03 (2008) 054.
[43] J. D. Brown and M. Henneaux, Central charges in the canonical realization of asymptotic symmetries: An example from three dimensional gravity, Commun. Math. Phys. **104**, 207 (1986).
[44] See Supplemental Material at http://link.aps.org/supplemental/10.1103/PhysRevB.109.L041104 for more details about the holographic and lattice calculations.
[45] J. Maldacena, The large-N limit of superconformal field theories and supergravity, Int. J. Theor. Phys. **38**, 1113 (1999).
[46] S. Gubser, I. Klebanov, and A. Polyakov, Gauge theory correlators from non-critical string theory, Phys. Lett. B **428**, 105 (1998).
[47] E. Witten, Anti-de Sitter space and holography, Adv. Theor. Math. Phys. **2**, 253 (1998).
[48] S. Coleman and F. De Luccia, Gravitational effects on and of vacuum decay, Phys. Rev. D **21**, 3305 (1980).
[49] S. Ryu and T. Takayanagi, Holographic derivation of entanglement entropy from the anti–de Sitter space/conformal field theory correspondence, Phys. Rev. Lett. **96**, 181602 (2006).
[50] S. Ryu and T. Takayanagi, Aspects of holographic entanglement entropy, J. High Energy Phys. 08 (2006) 045.
[51] J. Cardy and E. Tonni, Entanglement Hamiltonians in two-dimensional conformal field theory, J. Stat. Mech. (2016) 123103.
[52] S. Dutta and T. Faulkner, A canonical purification for the entanglement wedge cross-section, J. High Energy Phys. 03 (2021) 178.
[53] J. Kudler-Flam, Y. Kusuki, and S. Ryu, The quasi-particle picture and its breakdown after local quenches: Mutual information, negativity, and reflected entropy, J. High Energy Phys. 03 (2021) 146.
[54] Y. Zou, K. Siva, T. Soejima, R. S. K. Mong, and M. P. Zaletel, Universal tripartite entanglement in one-dimensional many-body systems, Phys. Rev. Lett. **126**, 120501 (2021).
[55] Y. Kusuki and K. Tamaoka, Entanglement wedge cross section from CFT: Dynamics of local operator quench, J. High Energy Phys. 02 (2020) 017.
[56] C. Akers and P. Rath, Entanglement wedge cross sections require tripartite entanglement, J. High Energy Phys. 04 (2020) 208.
[57] J. Kudler-Flam, Y. Kusuki, and S. Ryu, Correlation measures and the entanglement wedge cross-section after quantum quenches in two-dimensional conformal field theories, J. High Energy Phys. 04 (2020) 074.
[58] P. Bueno and H. Casini, Reflected entropy, symmetries and free fermions, J. High Energy Phys. 05 (2020) 103.
[59] P. Bueno and H. Casini, Reflected entropy for free scalars, J. High Energy Phys. 11 (2020) 148.
[60] V. Chandrasekaran, M. Miyaji, and P. Rath, Including contributions from entanglement islands to the reflected entropy, Phys. Rev. D **102**, 086009 (2020).
[61] C. Berthiere, H. Chen, Y. Liu, and B. Chen, Topological reflected entropy in Chern-Simons theories, Phys. Rev. B **103**, 035149 (2021).
[62] T. Li, J. Chu, and Y. Zhou, Reflected entropy for an evaporating black hole, J. High Energy Phys. 11 (2020) 155.
[63] Z. Wei and Y. Yoneta, Counting atypical black hole microstates from entanglement wedges, arXiv:2211.11787.
[64] B. Czech, J. L. Karczmarek, F. Nogueira, and M. V. Raamsdonk, The gravity dual of a density matrix, Class. Quant. Grav. **29**, 155009 (2012).
[65] A. C. Wall, Maximin surfaces, and the strong subadditivity of the covariant holographic entanglement entropy, Class. Quant. Grav. **31**, 225007 (2014).
[66] M. Headrick, V. E. Hubeny, A. Lawrence, and M. Rangamani, Causality & holographic entanglement entropy, J. High Energy Phys. 12 (2014) 162.
[67] K. Umemoto and T. Takayanagi, Entanglement of purification through holographic duality, Nat. Phys. **14**, 573 (2018).
[68] P. Nguyen, T. Devakul, M. G. Halbasch, M. P. Zaletel, and B. Swingle, Entanglement of purification: From spin chains to holography, J. High Energy Phys. 01 (2018) 098.
[69] J. Kudler-Flam and S. Ryu, Entanglement negativity and minimal entanglement wedge cross sections in holographic theories, Phys. Rev. D **99**, 106014 (2019).
[70] K. Tamaoka, Entanglement wedge cross section from the dual density matrix, Phys. Rev. Lett. **122**, 141601 (2019).
[71] E. O'Brien and P. Fendley, Lattice supersymmetry and order-disorder coexistence in the tricritical Ising model, Phys. Rev. Lett. **120**, 206403 (2018).
[72] D. A. Huse, Exact exponents for infinitely many new multicritical points, Phys. Rev. B **30**, 3908 (1984).
[73] U. Schollwöck, The density-matrix renormalization group in the age of matrix product states, Ann. Phys. **326**, 96 (2011).
[74] I. Peschel, Calculation of reduced density matrices from correlation functions, J. Phys. A: Math. Gen. **36**, L205 (2003).
[75] I. Peschel and V. Eisler, Reduced density matrices and entanglement entropy in free lattice models, J. Phys. A: Math. Theor. **42**, 504003 (2009).

[76] S. R. White, Density matrix formulation for quantum renormalization groups, Phys. Rev. Lett. **69**, 2863 (1992).
[77] C. F. Uhlemann and M. Wang, Splitting interfaces in 4d $\mathcal{N} = 4$ SYM, J. High Energy Phys. 12 (2023) 053.
[78] A. Roy and H. Saleur, Entanglement entropy in the Ising model with topological defects, Phys. Rev. Lett. **128**, 090603 (2022).
[79] D. Rogerson, F. Pollmann, and A. Roy, Entanglement entropy and negativity in the Ising model with defects, J. High Energy Phys. 06 (2022) 165.
[80] A. Karch, Y. Kusuki, H. Ooguri, H.-Y. Sun, and M. Wang, Universality of effective central charge in interface CFTs, J. High Energy Phys. 11 (2023) 126.
[81] P. Hayden, O. Parrikar, and J. Sorce, The Markov gap for geometric reflected entropy, J. High Energy Phys. 10 (2021) 047.
[82] C. V. Cogburn, A. L. Fitzpatrick, and H. Geng, CFT and lattice correlators near an RG domain wall between minimal models, arXiv:2308.00737.
[83] A. Konechny, RG boundaries and interfaces in Ising field theory, J. Phys. A: Math. Theor. **50**, 145403 (2017).